

Comparative Study of Temperature Distribution on Various Roof Surfaces Due to Solar Insolation: Computer Simulation Approach

Dr. Shweta Manchanda¹ and Khushal Matai^{2*}

¹Associate Professor of Architecture, School of Planning and Architecture, New Delhi 110002, India

²Ph.D. Scholar, School of Planning and Architecture, New Delhi 110002, India

E-mail: *arkhushal@live.com

Abstract—This paper is focused on modeling of temperature distribution and its time evolution on and around the surfaces exposed to direct sunlight during different seasons. The simulation results would help in identifying the appropriate roof material for roofs to affect reduction in surface to ambient radiation. This will help in reducing localized heating of outdoor environment caused due to the surface heating. This paper emphasizes on the mathematical model for simulation of the temperature variation on surfaces with different emissive and reflective properties. A methodological simulation procedure using ambient data in the COMSOL Multiphysics modeling environment and spatial visualization of temperature profile is adopted. Computer simulation results are then used to assess the heat flux variation on three different surfaces- asphalt, concrete, cool roof, in the same ambient thermal conditions. It is observed that daytime summer surface temperatures of asphalt and concrete surface are 13°C and 04°C higher than cool roof surface respectively. whereas early night-time winter surface temperatures of cool roof are found to be lower than ambient air temperature. Therefore, it is established that only by changing the surface type, peak temperature levels can be decreased by 50%. This paper concludes with the findings that reflectivity and emissivity of a material's surface have strong influence on its surface temperature and near surface air temperature.

Keywords: Heat flux; COMSOL Multiphysics; computer simulation; 3D model; solar insolation; roof surfaces.

Introduction

Thermal emissivity of a material determines the amount of heat radiated per unit area at a given temperature. It determines the material's contribution to urban heat island effect. Albedo or solar reflectivity is another key thermal characteristic which indicates the reflecting power of a surface. It's a dimensionless fraction defined as a ratio of the reflected solar radiation to the incident solar radiation at the surface. Emissivity and albedo influence the heating and/or cooling process of a conventional surface. Albedo largely impacts the maximum surface temperatures and emissivity affects minimum temperatures (Gui, et al., 2007). Cool surfaces have high reflective properties, which helps in mitigating heat island effect. COMSOL Multiphysics is a finite element analysis, solver and Simulation software package for solving various physics and engineering applications. COMSOL Multiphysics software is used in various domains of science research and engineering calculation.

The first part of this paper briefly describes the theoretical background of the study and COMSOL Multiphysics software. The second part elaborates the modelling of the roof-surface and the thermal properties of all three different materials, followed by the comparative results on the behavioural variation of three different roof-surfaces in the same ambient climatic conditions. The simulations aim to assess the distribution of temperature on the roof surface and temperature variation in the air surrounding the roof surface due to heat flux caused by its thermo physical properties. Geometric model of the surface was made in COMSOL Multiphysics 5.5 (COMSOL, 1998-2019) and was simulated with the Heat Transfer in solids and fluids, surface-to-surface radiation and laminar flow physics. In addition, heat transfer due to surface to surface radiation and isothermal flow Multiphysics were coupled. The time dependent computation study using the finite element method is performed to numerically solve the modelled physics.

Model Description

The basic parameterised 3D model of the studied surface types was made in standard Model Builder of COMSOL Multiphysics. Its geometric layout is shown in Figure 1. The model basically includes two domains – solid and fluid, which influence heat transfer in surrounding outdoor environment. Solid domain consists of a roof-slab (Green colour) whereas fluid domain defines air domain (Blue colour), surrounding the roof-slab.

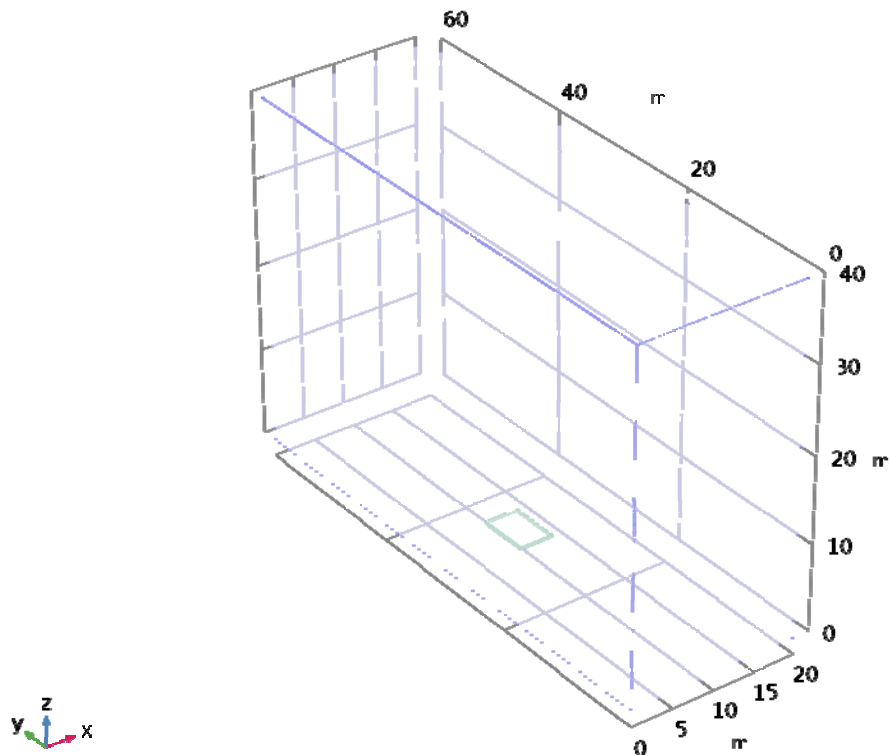


Figure 1: Geometric layout of the studied model

Simulation Conditions

Three case scenarios having different surface types were built and simulated with ASHRAE 2017 data file for 7 days during summer time, 2nd June 2019 and 7 days during winter time, 2nd January 2020. The three surface types used are – Asphalt, Concrete and Cool roof.

Data parameters

Meteorological data of station 421820 which is New Delhi Safdarjung, India (28.585° N, 77.206° E, 215 M) was the basis of ambient settings in the modelling software. Data parameters used were wind, relative humidity, temperature, humidity, pressure, and irradiance from ASHRAE 2017.

Material Properties

Size and material properties of the geometrical elements of the tested surface are listed in Table 1.

Additional conditions, geometry and material properties of the studied model include:

Table 1: Material Properties

Description	Asphalt surface	Concrete surface	Cool roof surface
Dimensions(m). [X;Y;Z]	4, 6, 0.3	4, 6, 0.3	4, 6, 0.3
Thermal Conductivity [W/(m.K)]	0.75	1.8	1.8
Density kg/m ³	-	2300	574
Specific Heat Capacity. [J/(kg.K)]	920	880	1100
Emissivity	0.94(Transportation, 2019)	0.92 (VanGeem, 2008)	0.9 (Eliane Coser, 2015)
Reflectivity	0.16(Transportation, 2019)	0.4(VanGeem, 2008)	0.52(Eliane Coser, 2015)
Absorption coefficient	0.84	0.6	0.48

Governing equations

Laminar flow

$$\rho \frac{\partial \mathbf{u}}{\partial t} + \rho(\mathbf{u} \cdot \nabla)\mathbf{u} = \nabla \cdot [-\rho\mathbf{I} + \mathbf{K}] + \mathbf{F} \quad (1)$$

$$\frac{\partial \rho}{\partial t} + \nabla \cdot (\rho\mathbf{u}) = 0 \quad (2)$$

$$\mathbf{K} = \mu(\nabla\mathbf{u} + (\nabla\mathbf{u})^T) - \frac{2}{3}\mu(\nabla \cdot \mathbf{u})\mathbf{I} \quad (3)$$

Heat transfer condition in Solid Domain

$$\rho C_p \frac{\partial T}{\partial t} + \rho C_p \mathbf{u} \cdot \nabla T + \nabla \cdot \mathbf{q} = Q + Q_{\text{rad}} \quad (4)$$

$$\mathbf{q} = -k\nabla T \quad (5)$$

Heat transfer condition in Fluid Domain

$$\rho C_p \frac{\partial T}{\partial t} + \rho C_p \mathbf{u} \cdot \nabla T + \nabla \cdot \mathbf{q} = Q + Q_p + Q_{\text{rad}} \quad (6)$$

$$\mathbf{q} = -k\nabla T \quad (7)$$

Heat Flux Equations

$$-\mathbf{n} \cdot \mathbf{q} = q_0 \quad (8)$$

$$q_0 = h(T_{\text{ext}} - T) \quad (9)$$

$$h = \begin{cases} \frac{k}{L} 0.54 Ra_L^{1/4} & \text{if } T > T_{\text{ext}} \text{ and } 10^4 \leq Ra_L \leq 10^7 \\ \frac{k}{L} 0.15 Ra_L^{1/3} & \text{if } T > T_{\text{ext}} \text{ and } 10^7 \leq Ra_L \leq 10^{11} \\ \frac{k}{L} 0.27 Ra_L^{1/4} & \text{if } T \leq T_{\text{ext}} \text{ and } 10^5 \leq Ra_L \leq 10^{10} \end{cases} \quad (10)$$

Surface to surface radiation

$$J = \epsilon e_b(T) + \rho_d G \quad (11)$$

$$G = G_m(J) + G_{\text{amb}} + G_{\text{ext}} \quad (12)$$

$$G_{\text{amb}} = F_{\text{amb}} e_b(T_{\text{amb}}) \quad (13)$$

$$e_b(T) = \sigma T^4 \quad (14)$$

Computer Model Construction

The basic geometric model of the roof surface was built in the standard Model Builder interface of COMSOL Multiphysics.

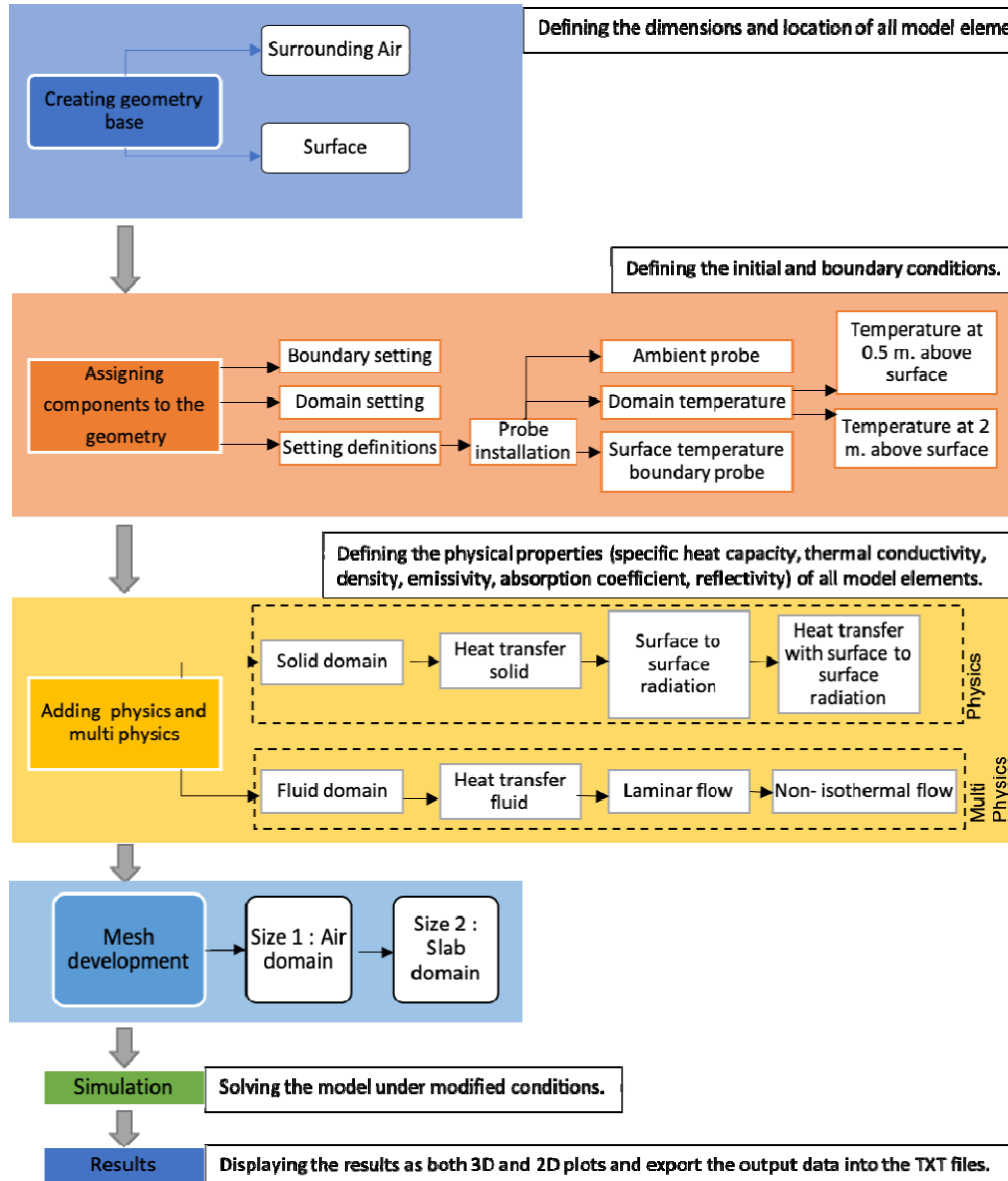


Figure 2: COMSOL simulation model

Simulation setup

Domain and boundary setting to the model

In the presented surface model, heat energy is transferred by convection and radiation. The convection describes heat transfer in the surrounding air due to radiative heating of roof surface. Thermal radiation is defined by the amount of emitted electromagnetic waves from a body at a certain temperature. For heat transfer in solids and fluids, solid (roof surface) domain and fluid (air) domain were assigned respectively. surface to surface radiation physics was applied on 5 boundaries of solid domain. Laminar flow physics was performed for fluid domain. Additionally, two Multiphysics non-isothermal flow and heat transfer due to surface to surface radiation were also applied in the model.

Mesh development

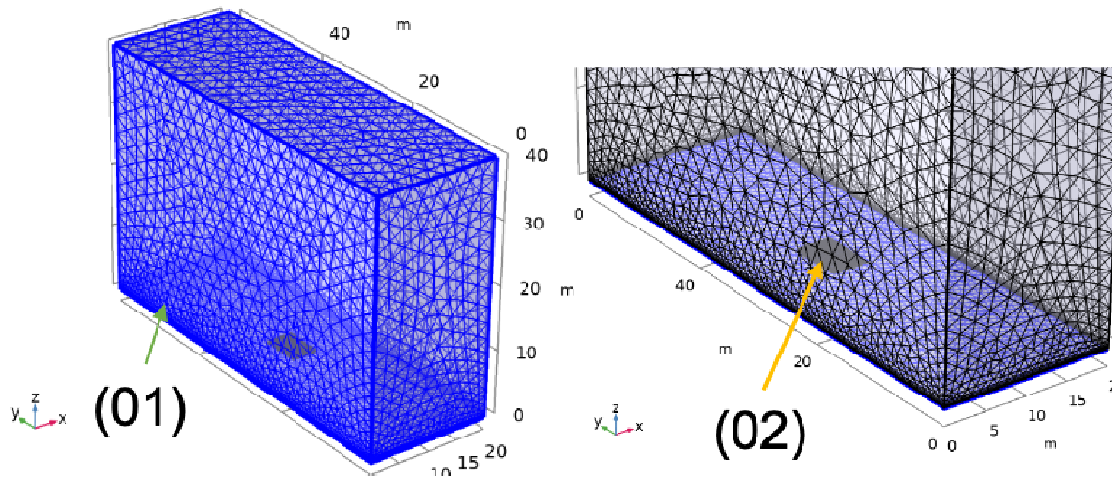


Figure 3: Meshed model: (01) view of air domain; (02) close-up view of solid surface.

A free tetrahedral mesh specified by a matrix of about 66,290 elements (degrees of freedom) was used to solve the finite element problem in the model environment. This matrix includes information about the physics, material property and boundary conditions based on the number of elements and the discretisation order. This way the size of this matrix is closely related to the complexity of the whole problem, demands for the size of computer memory, and time necessary for numerical modelling of the whole spatial model. The meshed model is shown in Figure 3. The average element quality of the used mesh was 0.6088, which is affected by the computational capacity. Considering the accuracy of the calculation, the simulation time and the available memory of the used computer, description of modelled mesh is shown in Table 2. Mesh density was set coarse and finer for fluid (air) domain and solid (surface) domain respectively.

Table 2: Mesh typology specifications

Description of Mesh	Size 01 (Air)	Size 02 (Roof Surface)
Mesh density	Coarse	Finer
Calibrate for	Fluid dynamics	General
Maximum element size (m)	2.83	3.3
Minimum element size (m)	0.849	0.24
Curvature factor	0.7	0.4
Resolution of narrow regions	0.6	0.7

The average simulation time for the selected sampling period of 168 hours i.e. 7days took around 10 hours. The model was calculated using COMSOL Multiphysics 5.5 on a computer with the Xeon processor Intel(R)CPU 2.90 GHz, 6 cores. The available memory was 63.5 GB. The whole simulation was performed by the PARADISO solver which is a part of the COMSOL Multiphysics software.

Results

The temperature fluctuations of all three surface types for the simulation period of summer (June 2-8) are being shown in Figure 4. The surface temperature and near-surface air temperatures at 2 levels ($T_{a@0.5m}$, $T_{a@2.0m}$) above surface are compared with meteorological temperature data.

Figure 4(a) shows that the asphalt surface has an overall higher temperature profile than the ambient temperature, which is 10°C more during the day and 15°C during the night. Whereas, the near surface air at a height of 0.5 m shows fluctuations but remain 4°C lower than the ambient temperature during day time. However, as the solar radiation decreases and the ambient temperature starts decreasing, the near surface temperature at the height of 0.5 m remains 4°C higher. The temperatures at 2 m above surface show small change over time.

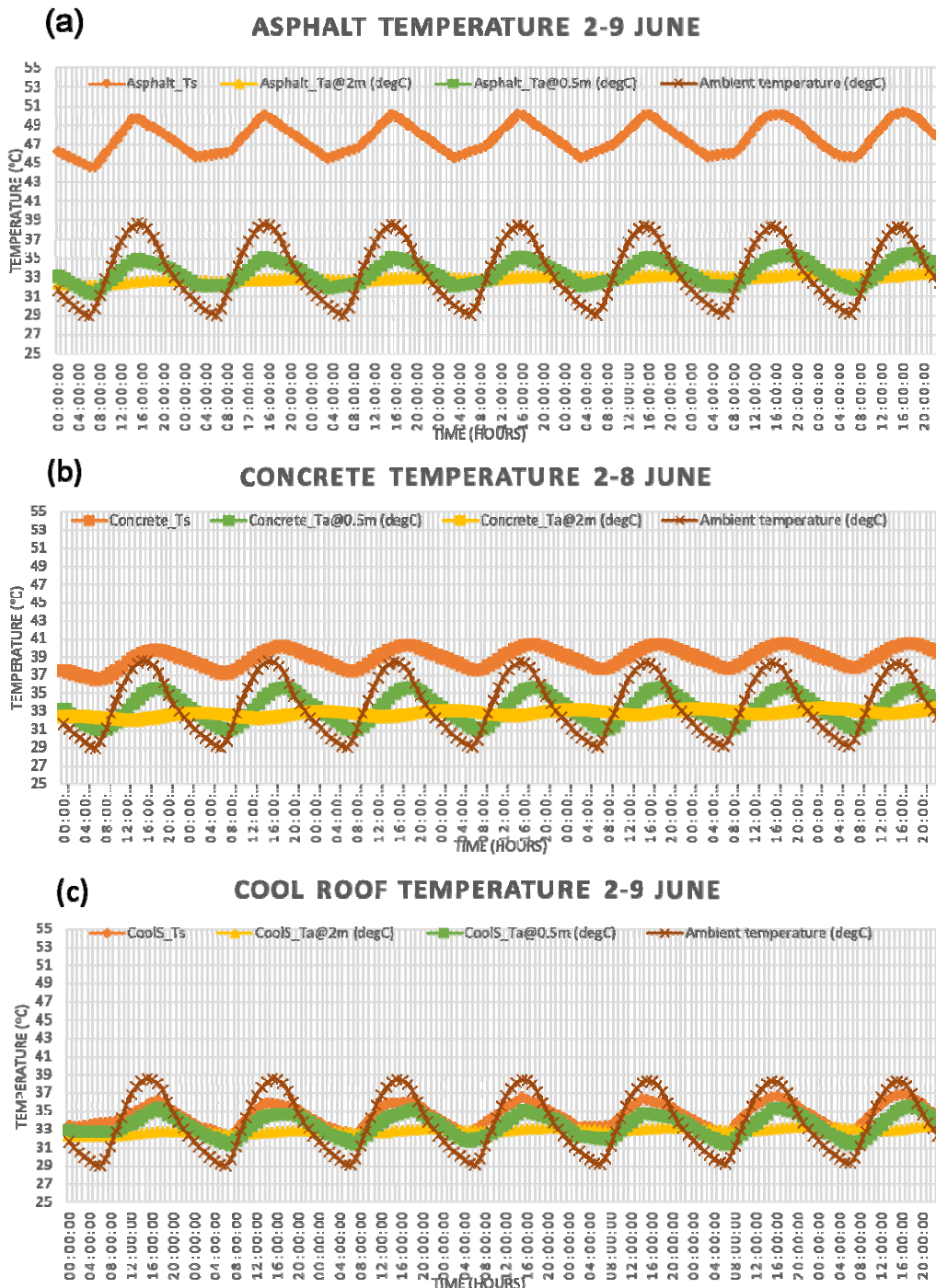


Figure 4: June (summer) temperature data (a) Asphalt; (b) Concrete; (c) Cool roof

Figure 4(b) demonstrates that the concrete surface has a gently undulating temperature profile which is 2°C higher than the peaks of the ambient temperature profile during the day time; whereas as the solar radiation decreases, the temperature starts decreasing but stays 9°C higher than the ambient temperature. Additionally, the highest and lowest temperature at the concrete surface follow the peak and low of the ambient temperature with a 2-3 hours' time lag. Whereas the temperature values at 2m have slight fluctuations and stay close to the average ambient temperature. Near surface temperature at 0.5m follows the ambient temperature profile but shows a -3°C and +2°C difference from the ambient temperature during day and night respectively.

Figure 4(c) shows that the surface temperature and both near-surface air temperature of the cool roof surface stay lower than the ambient temperature profile. The temperatures at the cool roof surface, and the near surface air temperature at a height of 0.5m almost overlap. Additionally the temperature profile of the cool roof surface show a -2.5°C and $+4^{\circ}\text{C}$ difference from the ambient temperature during day time and night time. Whereas, the temperature profile of the near surface air temperature show a -3°C and $+3^{\circ}\text{C}$ difference from the ambient temperature during day time and night time. The near surface temperature at 2 m do not rise and fall as extremely as the ambient temperature.

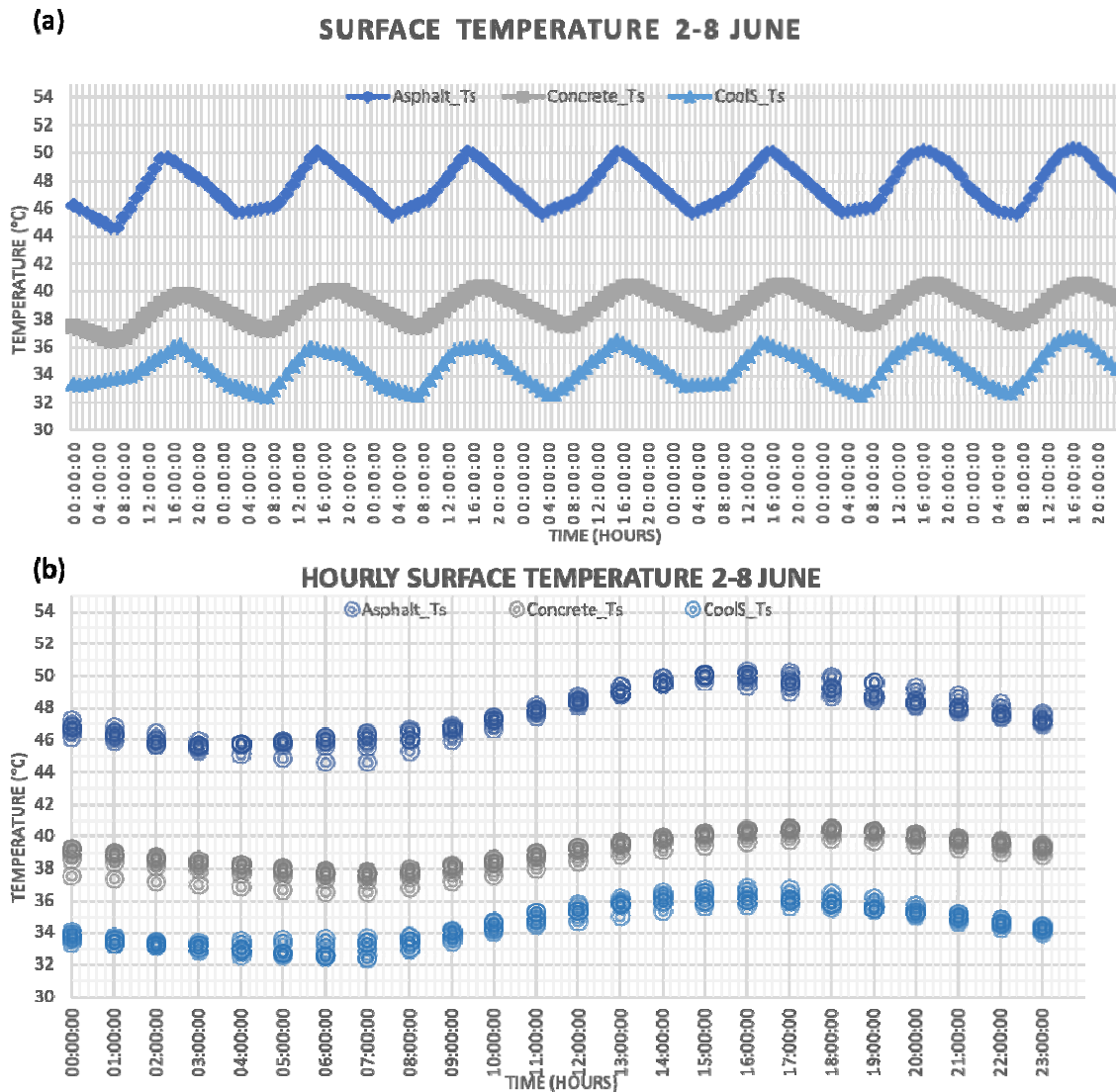


Figure 5: June (summer) surface temperature comparison (a) Daily; (b)Hourly

The overall temperature profile (Figure 5a) demonstrates that the values of asphalt surface are the highest and cool roof surface are the lowest in summers. Additionally, among all 3 surfaces, the temperature of asphalt surface remain most in sync with the rising solar insolation levels. Whereas, the other two surfaces i.e. concrete roof surface and cool roof surface show a time lag of 2 and 3 hours respectively.

The asphalt roof surface values show a steep increase with the increasing solar insolation values and a quick dip as the value of insolation decreases. The minimum and maximum temperature values for asphalt surface range between 44°C - 50°C (figure 5b). The concrete surface temperature demonstrates fluctuation between 40°C - 36°C (figure 5b) from day time to night time, with a gradual increase and decrease in values compared to the variations in the asphalt surface. The temperature of cool roof surface

starts rising around 9000 hours whereas the temperature of asphalt roof surface starts rising as quickly as the solar radiation starts increasing which is at 0700 hours. The minimum and maximum temperature values for cool roof surface range between 32°C-36°C (figure 5b). The cool roof surface temperature profile is similar to asphalt surface as the increase in the temperature is quite steep. However, the temperature starts decreasing at 1600 hours whereas the asphalt surface temperature starts decreasing at 1400 hours.

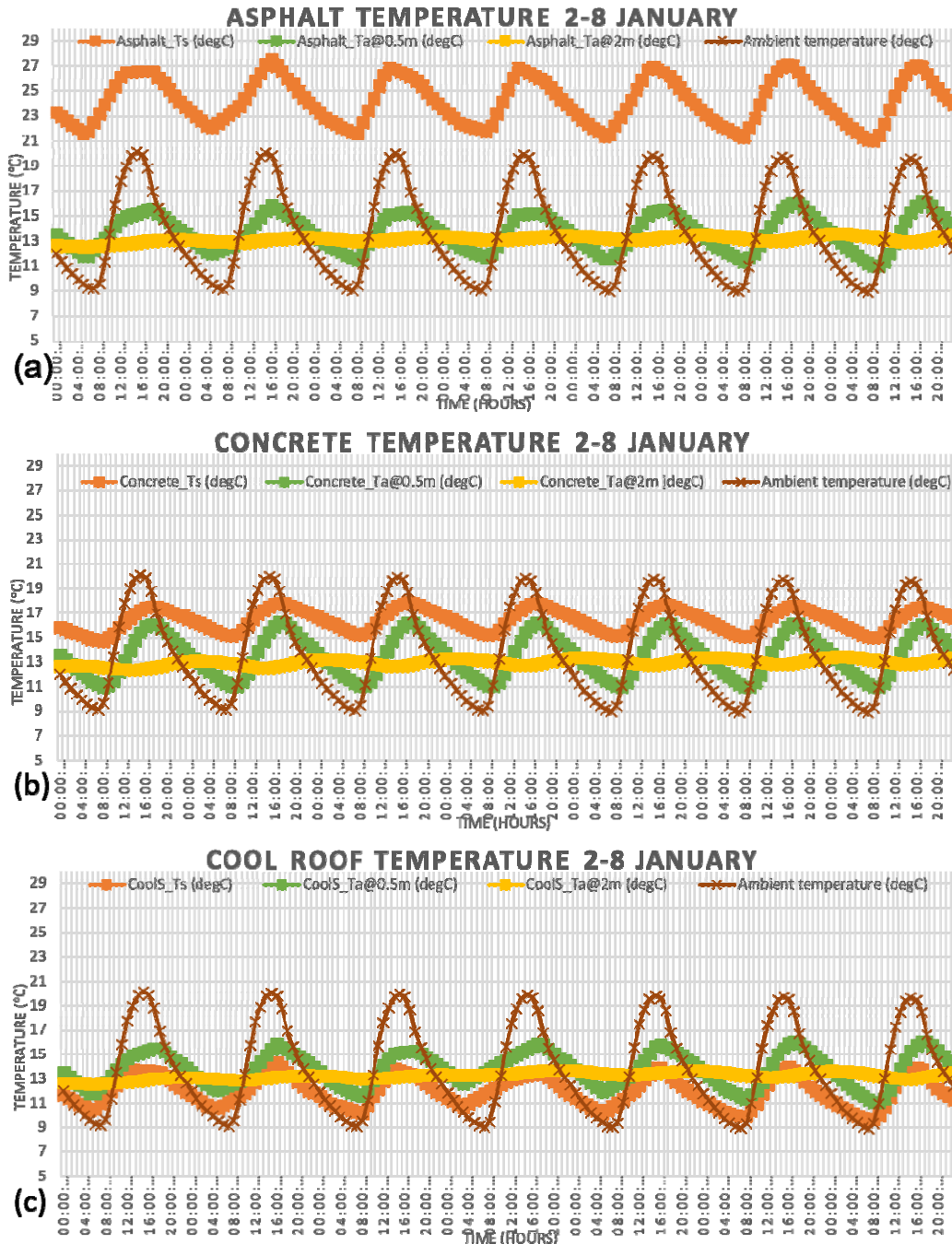


Figure 6: January (winter) temperature data (a) Asphalt; (b) Concrete; (c) Cool roof

The temperature fluctuations of all three surface types for the simulation period of winter time (January 2-8) are being shown in Figure 6. The surface temperature and near-surface air temperatures at 2 levels ($T_{a@0.5m}$, $T_{a@2.0m}$) above surface are compared with meteorological temperature data.

Figure 6(a) shows that the asphalt surface has an overall higher temperature profile than the ambient temperature, which is 7°C more during the day and 12°C during the night. Whereas, the near surface air at a height of 0.5 m shows fluctuations but remain 4°C lower than the ambient temperature during day time. However, as the solar radiation decreases and the ambient temperature starts decreasing, the near surface temperature at the height of 0.5 m remains 3°C higher. The temperatures at 2 m above surface show small change over time within a range of 1°C.

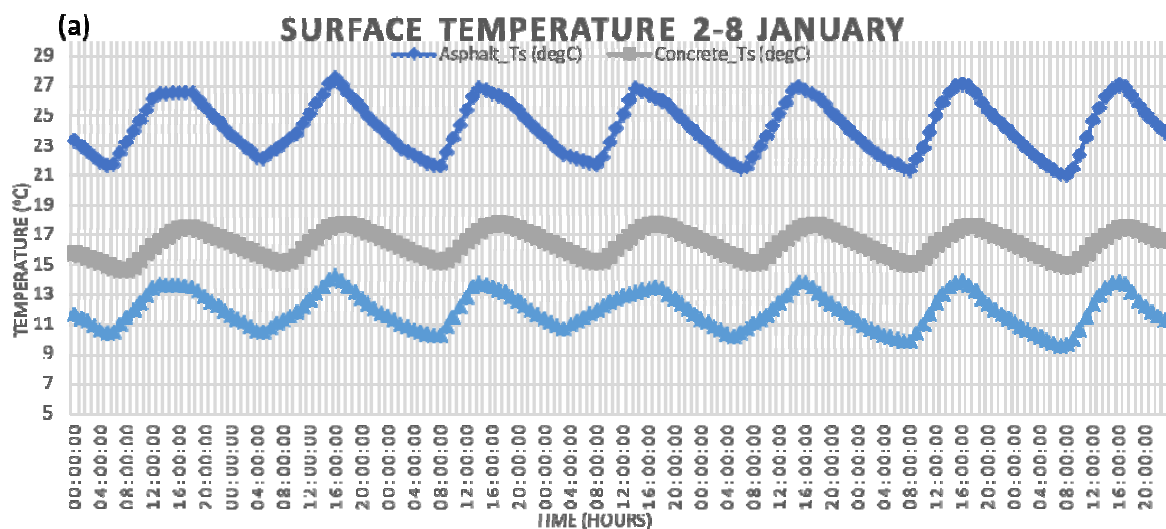
Figure 6(b) demonstrates that the concrete surface has a gently undulating temperature profile like summers. However, in winters the peaks are 2.5°C lower than the peaks of the ambient temperature profile during the day time; whereas as the solar radiation decreases, the temperature starts decreasing but stays 6°C higher than the ambient temperature. Additionally, the highest and lowest temperature at the concrete surface follow the peak and low of the ambient temperature with a 3-3.5 hours' time lag. Whereas the temperature values at 2m have slight fluctuations and stay close to the average ambient temperature within the range of 1°C. Near surface temperature at 0.5m follows the ambient temperature profile but shows a -4°C and +2°C difference from the ambient temperature during day and night respectively.

Figure 6(c) shows that the surface temperature and both near-surface air temperature of the cool roof surface stay lower than the ambient temperature profile in the winter as well. The temperature profile of cool roof surface and the near surface air temperature at a height of 0.5m have slight variations during daytime whereas they behave similarly at night time. Additionally the temperature profile of the cool roof surface show a 2°C difference from the near surface air temperature at a height of 0.5m. The temperature of cool roof surface shows a difference of - 6 °C and +2°C difference from the ambient temperature during day time and night time. Whereas, the temperature profile of the near surface air temperature at a height of 0.5m show a -4°C and +3°C difference from the ambient temperature during day time and night time respectively. The near surface temperature at 2 m remains mostly constant with minor variation of 0.5°C.

The overall temperature profile(Figure 7a) demonstrates that the values of asphalt surface are the highest and cool roof surface are the lowest in winters as well. However, with respect to the summer data, here, the temperature of asphalt surface as well as cool roof surface remain in sync with the rising solar insolation levels. Whereas, the concrete roof surface shows a time lag of 3 hours.

The asphalt roof surface values show a steep increase with the increasing solar insolation values and a slower dip, as compared to the summer trend, as the value of insolation decreases. The minimum and maximum temperature values for asphalt surface range between 21°C-27°C (figure 7b). The concrete surface temperature demonstrates fluctuation between 18°C- 14°C (figure 7b) from day time to night time, with a gradual increase and decrease in values compared to the variations in the asphalt surface. However, the trend is similar to the other 2 surfaces in a manner that the increase in values is steep whereas the decrease is slower .

The minimum and maximum temperature values for asphalt surface range between 10°C-13°C (figure 7b). The cool roof surface temperature profile is almost identical to asphalt surface as the increase in the temperature is quite steep. However, the maximum and minimum temperature of cool roof surface is half of the asphalt maximum and minimum temperature values.



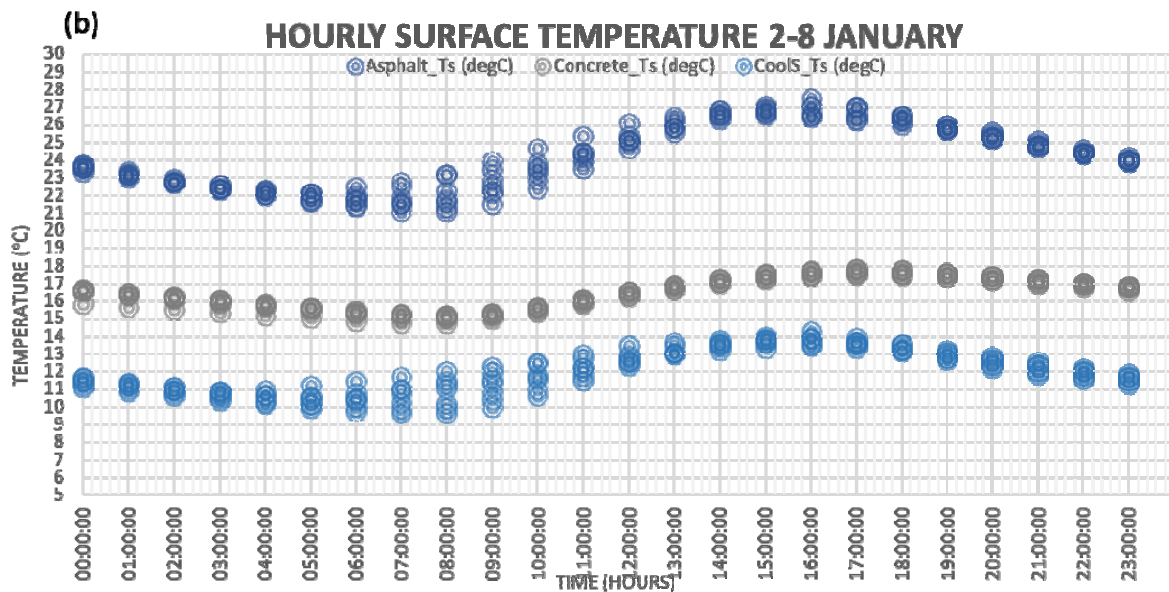


Figure 7: January (winter) surface temperature comparison (a) Daily; (b)Hourly

Discussion and Conclusions

It is observed that among all 3 surfaces, the temperature of asphalt surface remain most in sync with the rising solar insolation levels in summers and winter both. Additionally, the temperature of asphalt surface remain higher than other 2 surfaces in summers and winters. Due to low reflectivity and high specific heat capacity, most of the solar radiation is absorbed and stored in the thermal mass of asphalt surface. This absorbed heat is re-radiated gradually due to the high emissivity and low thermal conductivity values of the material. The high density of the concrete surface aids in holding the absorbed heat and releasing it gradually back to the atmosphere. The high reflectivity properties of the cool roof surface cause delayed yet steep increase in the temperature but a faster decrease as the surface reradiates most heat back into the surroundings due to its high emissivity. In winters, all 3 surfaces reach their thermal capacity peak slower than the summer time so the decrease in temperature is gradual during winter than summers.

The temporal profiles of near-surface air show a similar trend to that of ambient air temperature in case of all three asphalt, concrete and cool surfaces. The difference between ambient and near surface temperature declines consecutively from asphalt, concrete to cool roof in both summer and winter. It is evident from the findings that the near-surface air temperatures during summer days diminish gradually as the height above the surface increases. Gradually temperature profile also stops changing. This shows that the spatial profiles of near-surface air temperature are influenced by the surface temperature, ambient air temperature, and wind speed. Low wind speeds make the spatial profiles steeper owing to less heat dissipated by air movement. Hence, it is worth noticing that the heat flux in the high density urban areas with low wind speed will increase the surrounding temperatures.

Findings obtained from the simulation indicate that the reflectivity of the surface influence the temperature levels of both; the surface as well as air near the surface. The temperatures also show relatively high sensitivity to thermal emissivity, convection coefficient and thermal conductivity due to wind flow. Remaining material properties such as, specific heat capacity and density pose low to no effect on surface temperature and near surface air temperature, respectively. This clearly indicates that the temperature of any surface exposed to solar insolation can be reduced by increasing its solar reflectivity. However, the effect of high-reflective roof surface on global albedo levels is unknown and needs to be explored. According to the identified factors based on the comparison, surface with high reflectivity could be an effective measure to reduce heat flux in the outdoor environment. Effect of shading on the roof surface temperature will be explored in future work. Another observation evident from the results is that the usage of cool roof technology keeps surface temperature low, not only in June (summers) but also in January (winters) for most of the hours of simulated days. Therefore, it is important to mention the potential occurrence of harsh effects during cold seasons, especially during night time. This leads to the probability of more comprehensive research in both technology and technique of cool roof surfaces.

Conflicts of Interest: The authors declare no conflict of interest.

Abbreviations

The following symbols are used in this paper:

t	Time [h]
ρ	density (kg/m ³)
h	Heat transfer coefficient [$\text{W} \cdot \text{m}^{-2} \text{K}^{-1}$]
cp	Specific heat capacity [$\text{J} \cdot \text{K}^{-1}$]
n	Normal vector
Q	additional heat sources [W/m ³]
q	Heat flow density [$\text{W} \cdot \text{m}^{-2}$]
qr	Incident radiant heat flow per unit surface area [$\text{W} \cdot \text{m}^{-2}$]
qs	Heat flow density on the surface [$\text{W} \cdot \text{m}^{-2}$]
λ	Thermal conductivity [$\text{W} \cdot \text{m}^{-1} \text{K}^{-1}$]
T	Absolute Temperature [K]
Tamb	Ambient temperature [K]
Tinf	External temperature [K]
Te	Convective exchange temperature [K]
Ts	Surface temperature [K]
T0	Initial temperature of a body [K]
p	pressure [Pa]
τ	viscous stress tensor [Pa]
u	velocity vector [$\text{m} \cdot \text{s}^{-1}$]
v	Fluid velocity [$\text{m} \cdot \text{s}^{-1}$]
x, y, z	Space coordinates [m]
α	coefficient of thermal expansion[1/K]
S	second Piola-Kirchhoff stress tensor [Pa]
ϵ	Emissivity
σ	Stephan–Boltzmann constant, $\sigma = 5.670367 \cdot 10^{-8} \text{ W} \cdot \text{m}^{-2} \text{K}^{-4}$

References

- [1] Gui, J. _, Phelan, P. E., Kaloush, K. E. & Golden, a. J. S., 2007. Impact of Pavement Thermophysical Properties on Surface Temperatures. *JOURNAL OF MATERIALS IN CIVIL ENGINEERING*, Volume 19, pp. 683-690.
- [2] COMSOL, 1998-2019. *Introduction to COMSOL Multiphysics*. [Online] Available at: <https://cdn.comsol.com/doc/5.5/IntroductionToCOMSOLMultiphysics.pdf> [Accessed January 2020].
- [3] Eliane Coser, V. F. M. A. K. a. C. A. F., 2015. Development of paints with infrared radiation reflective properties. *Scientific Technical*, 25(3), pp. 305-310.
- [4] VanGeem, M. L. M. a. M. G., 2008. *Solar Reflectance Values of Concrete*, s.l.: Portland Cement Association.
- [5] Transportation, U. D. o., 2019. *Pavement Thermal Performance And Contribution To Urban And Global Climate*. [Online] Available at: https://www.fhwa.dot.gov/pavement/sustainability/articles/pavement_thermal.cfm [Accessed 15 02 2020].